Received: 10 April 2018 | Revised: 2 September 2018 | Accepted: 29 October 2018

DOI: 10.1002/sia.6588

WILEY SURFACE and INTERFACE ANALYSIS

RESEARCH ARTICLE

Tribological properties of Ti-doped diamond-like carbon coatings under dry friction and PAO oil lubrication

Youzhi Guo[1,2] | Peng Guo[1] | Lili Sun[1] | Xiaowei Li[1,3] | Peiling Ke[1] | Qiang Li[2] | Aiying Wang[1]

[1] Key Laboratory of Marine Materials and Related Technologies, Zhejiang Key Laboratory of Marine Materials and Protective Technologies, Ningbo Institute of Materials Technology and Engineering, Chinese Academy of Sciences, Ningbo, China

[2] School of Materials Science and Engineering, Shanghai University, Shanghai, China

[3] Computational Science Center, Korea Institute of Science and Technology, Seoul, Republic of Korea

Correspondence
Aiying Wang, Key Laboratory of Marine Materials and Related Technologies, Zhejiang Key Laboratory of Marine Materials and Protective Technologies, Ningbo Institute of Materials Technology and Engineering, Chinese Academy of Sciences, Ningbo 315201, China.
Email: aywang@nimte.ac.cns

Funding information
National Natural Science Foundation of China, Grant/Award Numbers: 51522106 and 51601211; Zhejiang Key Research and Development Program, Grant/Award Number: 2017C01001; Chinese Academy of Sciences President's International Fellowship Initiative, Grant/Award Number: 2018VEA0007; National Key R&D Program of China, Grant/Award Number: 2017YFB0702303

Titanium-doped diamond-like carbon (Ti-DLC) coatings with Ti concentration of 4 at.% ($Ti_{4at.\%}$-DLC) and 27 at.% ($Ti_{27at.\%}$-DLC) were prepared by a hybrid ion beam deposition system for comparison. The tribological behaviors of Ti-DLC coatings under dry friction and boundary lubrication conditions were systematically investigated. Results showed that, under dry friction, the $Ti_{4at.\%}$-DLC coating displayed lower friction coefficient (0.07) and wear rate due to the continuous transfer film formed in the sliding interface, while $Ti_{27at.\%}$-DLC coating was worn out at initial stage due to severe abrasive wear. And under boundary lubrication, both the $Ti_{4at.\%}$-DLC and $Ti_{27at.\%}$-DLC coatings showed excellent tribological properties attributing to the formation of oil film between sliding interface. In particular, $Ti_{27at.\%}$-DLC performed the lowest wear rate of 1.12×10^{-16} m^3 N^{-1} m^{-1} in this friction case. In conclusion, compared with $Ti_{27at.\%}$-DLC coating, $Ti_{4at.\%}$-DLC coating exhibited better tribological performances both under dry friction and boundary lubrication. The present result provides guidance for the selection of DLC coatings according to the realistic environment of starved-oil and rich-oil conditions.

KEYWORDS

diamond-like carbon, dry friction, lubrication mechanism, oil lubrication, Ti doped, transfer film

1 | INTRODUCTION

With the development of industrial technology, some engine components have to serve in harsh conditions, such as high speeds and rigorous loads.[1,2] To improve the stability and safety of components, liquid lubricants are usually adopted to solve the wear replenishment problem and remove the wear debris during the friction process. However, in practical engineering application, starved-oil lubrication is a universal and unavoidable issue, leading to the lubrication failure of protective surface.[3] Combining solid lubrication coating with liquid lubricating oil is an effective strategy to achieve the long-term reliability of various engines.

Taking advantages of the excellent self-lubricating properties and superior mechanical performance, diamond-like carbon (DLC) has become one of the promising candidates to be used as solid lubrication coating.[4,5] Especially, metal-doped DLC (Me-DLC) coating has been given much attention because metal doping could not only reduce the intrinsic high residual stress of DLC coating, but also improve the tribological properties and adhesion strength to metallic substrate.[6-9] Among of various Me-DLC coatings, Ti-DLC coatings showed the most promising benefits with the enhancement of abovementioned properties.[10-12] In addition, previous study also proved that the microstructure of Ti-DLC coating was closely related to the doping content. With proper titanium content, a small number of TiC nanocrystallites would be distributed in the DLC matrix, which can endow Ti-DLC coatings with higher hardness and elastic modulus,[6,13] that is one key issue for the application of solid lubrication coating.

Recently, many researches have focused on the interaction between the DLC coatings and lubricating oil (mainly base oil poly-

alpha-olefin (PAO), extreme-pressure additives, and friction-modifier additives) to explore the solid-liquid composite lubrication behavior.[14-17] For example, Kano et al[18] reported that ultralow friction coefficient (0.03) was obtained by sliding hydrogen-free tetrahedral amorphous carbon (ta-C) against ta-C when PAO containing glycerol mono-oleate additive was used as lubricant, and revealed that the formation of OH^- terminated DLC surface was the key factor to this friction phenomena. However, Gorbatchev et al[17] observed that dithiocarbamates reduced friction and wear for DLC/DLC mating contact, but its lubrication effect faded due to the severe chemical wear for DLC/steel contact surface. As to Ti-DLC coating, some studies also showed low friction and wear under oil lubrication condition. de Barros'Bouchet[19] reported that Ti-DLC/Ti-DLC contact lubricated with PAO base oil resulted in slightly lower friction and wear than the nondoped DLC/DLC. Considering the higher reactivity with oils of Ti-DLC coating, Kalin[20] reported that Ti-DLC boundary lubrication was promoted via binding sites at O vacancies present in the Ti-DLC coating due to oxidation of Ti. Furthermore, Ti-DLC coating showed higher friction with base oil only, and addition of additives always further reduced the friction.[21] However, the tribological property of Ti-DLC/lubricating oil depends on the structure of Ti-DLC coating, kinds of lubricants, and friction-induced interfacial reaction, which involves multiple factors and is quite complicated; how the microstructure affects the friction and wear process is unclear. So, comprehensive studies on its tribological behaviors under both dry friction and boundary lubrication are of great importance to optimize the DLC/lubricating oil systems for practical engineering application, especially for the engine components working in both starved-oil and rich-oil lubrication conditions.

In the present study, Ti-DLC coatings with different microstructures were designed and prepared by a hybrid ion beam deposition system, namely one sample with Ti atoms dissolved in the DLC matrix at low (4 at.%) concentration and the other one with titanium carbide nanocrystallites at high Ti (27 at.%) concentration. The widely used base oil PAO was chosen as lubricant. The tribological properties of Ti-DLC coatings under both dry friction and boundary lubrication conditions were studied, and related lubrication mechanism was discussed in terms of the microstructural evolution and transfer film formed during the friction sliding.

2 | EXPERIMENTAL DETAILS

Ti-DLC coatings were deposited by a hybrid ion beam deposition system consisting of a rectangular DC magnetron sputtering source with a Ti target (99.99%) and a linear anode-layer ion sources (LIS). Figure 1 shows the schematic diagram of used deposition system. Prior to deposition, single crystal P(100) silicon substrates were ultrasonically cleaned in acetone for 15 minutes and then etched in Ar plasma for 10 minutes to remove the surface contaminations. Then, precursor gases C_2H_2 (from ion source) at 10 sccm and Ar (from sputtering source) at 70 sccm were introduced into the chamber to deposit Ti-DLC coatings. Typical values of LIS voltage and current were 1500 V and 0.2 A, respectively. Ti content in the coatings was controlled by adjusting DC sputtering current. The DC pulsed negative bias of −100 V with a frequency of 350 kHz was applied to the substrate during etching and deposition process. The thickness of Ti-DLC coatings was kept at 520 ± 20 nm by changing deposition time. The target-substrate distance was strictly controlled at 20 cm, and all samples were deposited at room temperature. Deposition parameters and properties of Ti-DLC coatings in this study are listed in Table 1, where samples deposited at 2.0 and 3.5 A were named $Ti_{4at.\%}$-DLC and $Ti_{27at.\%}$-DLC, respectively.

The friction tests were carried out using a reciprocating ball-on-disk tribometer (Figure 2) under 5 N load, at velocity of 0.05 m second^{-1} for a total distance of 90 m, with GCr15 steel ball (Φ 6 mm, Ra = 0.05 μm) as sliding friction pair. Test temperature and humidity were 25°C and 70% RH, respectively. In order to keep verification and reproducibility of results, the tests were repeated at least three times for each condition.

The theoretical minimum film thickness (h_{min}) and dimensionless lambda ratio (λ) were calculated using Equations 1 and 2, respectively, to ensure a boundary lubricated regime.

$$h_{min} = 3.63RU^{0.68}G^{0.49}W^{-0.073}\left(1 - e^{-0.68k}\right) \quad (1)$$

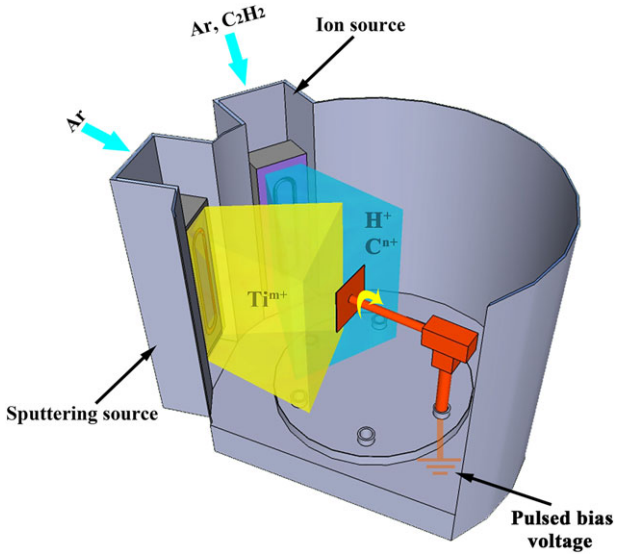

FIGURE 1 Schematic diagram of the hybrid ion beam deposition system

TABLE 1 Deposition parameters and characteristics of Ti-DLC coatings

Sample	Target Substrate Distance, cm	Deposition Temperature	DC Sputtering Current, A	Substrate Bias, V	Deposition Time, min	Ti Content, at%	Thickness, nm	Hardness, GPa	Elasticity Modulus, GPa	H/E	H^3/E^2
$Ti_{4at.\%}$-DLC	20	RT	2.0	−100	25	4	509	16.80	158.28	0.11	0.19
$Ti_{27at.\%}$-DLC	20	RT	3.5	−100	33	27	516	23.55	221.52	0.11	0.27

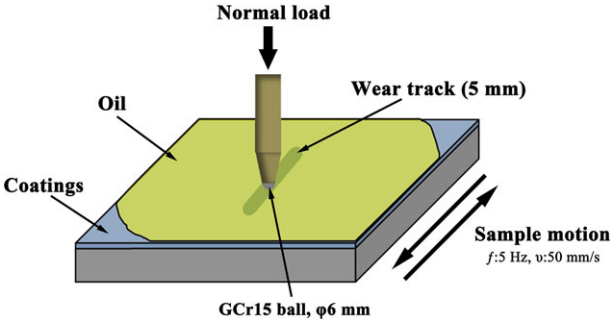

FIGURE 2 Schematic diagram of reciprocating ball-on-disk tribotest

$$\lambda = \frac{h_{\min}}{\sqrt{R_{q,a}^2 + R_{q,b}^2}} \tag{2}$$

where R is the radius of the ball, U is a dimensionless speed parameter, G is a dimensionless coating parameter, W is a dimensionless load parameter, $R_{q,a}$ is the surface roughness of the coating, and $R_{q,b}$ is the surface roughness of the ball. The calculated lambda parameters were 0.33 and 0.12, respectively, which stated that lubrication regime was boundary lubrication.

During testing, the friction coefficient was monitored continuously. After testing, the profile of wear track was measured by a surface profilometer (Alpha-Step IQ, USA); the volume of the removed coatings ($V_{coating}$) and steel ball (V_{ball}) was calculated using Equations 3 and 4, respectively.

$$V_{coating} = SL \tag{3}$$

$$V_{ball} = \frac{\pi^* \left[2R^3 - \left(2R^2 + r^2\right)\sqrt{R^2 - r^2}\right]}{3} \tag{4}$$

where S and L are sectional area and length of wear track, respectively, and r is the radius of wear scar.

The wear rates were calculated using Archard wear equation.[22,23]

$$k = V / Fs \tag{5}$$

where k is the wear rate ($m^3\ N^{-1}\ m^{-1}$), V is the wear volume (m^3), F is the normal load (N), and s is the total sliding distance. The morphology, chemical composition, and chemical bonds of wear tracks and wear scars were systematically analyzed and compared with as-deposited coatings. Specially, after oil lubrication tests, both Ti-DLC coatings and steel balls were immersed in *n*-hexane to remove adsorbed oil before characterization.

Mechanical properties were measured by the nanoindentation technique (MTS-G200) in a continuous stiffness measurement mode with a maximal indentation depth of 250 nm. A three pyramid diamond indentor with a tip ratio of 20 nm was used. The characteristic hardness of deposited coatings was chosen in the depth where the hardness with indentation depth was just stable and not affected by the substrate. And six replicate indentations were done for each sample.

Scanning electron microscopy (SEM, S-4800, Hitachi, Japan) was applied to investigate morphology of wear tracks and wear scars. Raman spectroscopy (Renishaw inVia-reflex, UK) with a laser wavelength of 532 nm was used to measure the atomic bonds of sample before and after tribological test, with the laser power 1.2 mW and detecting range from 800 to 2000 cm^{-1}. The experimental spectrum was fitted using two Gaussian peaks after background correction. X-ray photoelectron spectroscopy (XPS, Axis ultradld, Japan) with Al (monochromatic) Kα irradiation at a pass energy of 160 eV was used to characterize the chemical bonds of the transfer films on the wear scars. Charge neutralization was used, and the binding energies were referenced to C 1s at 284.6 eV. Peak fits were performed with the CasaXPS software package, after the subtraction of a Shirley background and with mixed Gaussian-Lorentzian curves. High-resolution transmission electron microscopy (HRTEM, FEI Tecnai F20, USA) was applied to characterize the microstructure of as-deposited coatings, which was operated at 200 kV with a pointed-to-point resolution of 0.24 nm.

3 | RESULT AND DISCUSSION

3.1 | Microstructural evolution of as-deposited coatings

Previous studies of Ti-DLC coatings have proved that the doped Ti content affected the microstructure significantly, which can change the tribological behaviors.[6,24] Figure 3 showed the microstructural evolution of deposited Ti-DLC coatings by HRTEM and selected area electron diffraction (SAED). In case of $Ti_{4at.\%}$-DLC coating, no crystalline phase could be found in the HRTEM image, as shown in

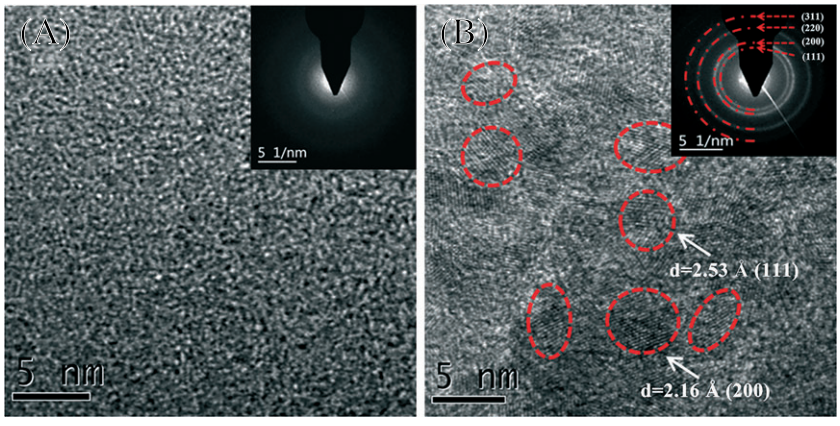

FIGURE 3 HRTEM images of (A) $Ti_{4at.\%}$-DLC and (B) $Ti_{27at.\%}$-DLC coatings

Figure 3A. The corresponding SAED just showed a diffused ring, indicating that doped titanium was uniformly dissolved in amorphous carbon matrix. However, for $Ti_{27at.\%}$-DLC coating, many nanocrystallites with size around 4~6 nm (labeled by red circle in Figure 3B) appeared in the amorphous carbon matrix. Moreover, the nanocrystalline diffraction patterns of the insert SAED were identified to (111), (200), (220), and (311) reflections of TiC (PDF#32-1383), respectively, demonstrating that the TiC nanoparticles were formed and embedded into DLC matrix.

3.2 | Friction and wear behavior

Figure 4A shows the friction coefficient of $Ti_{4at.\%}$-DLC and $Ti_{27at.\%}$-DLC coatings under dry friction and oil lubrication, respectively. Figure 4B is the close view of the first 300 seconds of the friction coefficient curve. When tested under dry frication, $Ti_{4at.\%}$-DLC coating exhibited a run-in period (about 300 seconds), then reached the lowest and stable friction with average friction coefficient 0.07. For the $Ti_{27at.\%}$-DLC coating, the friction coefficient curve showed obvious fluctuation phenomenon during a much longer run-in period (about 600 seconds), and it was almost entirely worn out after 10 minutes. However, when the PAO oil was used during the friction sliding, both $Ti_{4at.\%}$-DLC and $Ti_{27at.\%}$-DLC coatings illustrated low and stable friction curve, in which the average friction coefficient was around 0.09~0.13 and no distinct run-in period was visible. Figure 4C shows the wear rates of $Ti_{4at.\%}$-DLC and $Ti_{27at.\%}$-DLC coatings for comparison. The $Ti_{4at.\%}$-DLC coating exhibited high wear resistance under both dry friction and oil lubrication, with corresponding wear rate about 2.15×10^{-16} m^3 N^{-1} m^{-1} and 1.60×10^{-16} m^3 N^{-1} m^{-1}, respectively. However, the $Ti_{27at.\%}$-DLC coating displayed obviously different behaviors. Under dry friction, the coating failured rapidly and the wear rate could not be achieved. But the wear rate of $Ti_{27at.\%}$-DLC coating was significantly reduced to the lowest value of 1.12×10^{-16} m^3 N^{-1} m^{-1} under oil lubrication condition. Figure 4D shows the wear rates of corresponding GCr15 steel balls; under both conditions, the balls against $Ti_{4at.\%}$-DLC coating exhibited lower wear rate, and the lowest wear rate of 1.26×10^{-17} m^3 N^{-1} m^{-1} was obtained under oil lubrication. While the balls against $Ti_{27at.\%}$-DLC coating showed serious wear, especially under dry friction, which had the highest wear rate of 3.52×10^{-16} m^3 N^{-1} m^{-1}.

3.3 | Wear track and wear scar analysis

In order to clarify related lubrication mechanism, the morphology, component, and structure of wear tracks on coating surface and wear scars on steel ball were systematically analyzed. Figure 5 shows the SEM micrographs of wear tracks, and the illustrations were cross-sectional profiles of the wear tracks. For $Ti_{4at.\%}$-DLC coatings, the wear tracks obtained under both dry friction (Figure 5A) and oil lubrication (Figure 5D) conditions were very narrow. Moreover, almost no debris could be observed both inside and outside of wear tracks. Nevertheless, for $Ti_{27at.\%}$-DLC coating, complete delamination on the wear track surface occurred when tested under dry friction, as shown in Figure 5B. Figure 5C shows the corresponding EDS mapping image, which confirmed that no C and Ti but distinct Si element emerged in the wear track area. When tested under oil lubrication, as shown in Figure 5E and 5F, the wear track was still covered with DLC coatings, suggesting that after adding PAO oil, the wear resistance of $Ti_{27at.\%}$-DLC coating was improved obviously.

Raman spectroscopy was used to characterize evolution of carbon atomic bonds on the surface of the coatings and steel balls before and

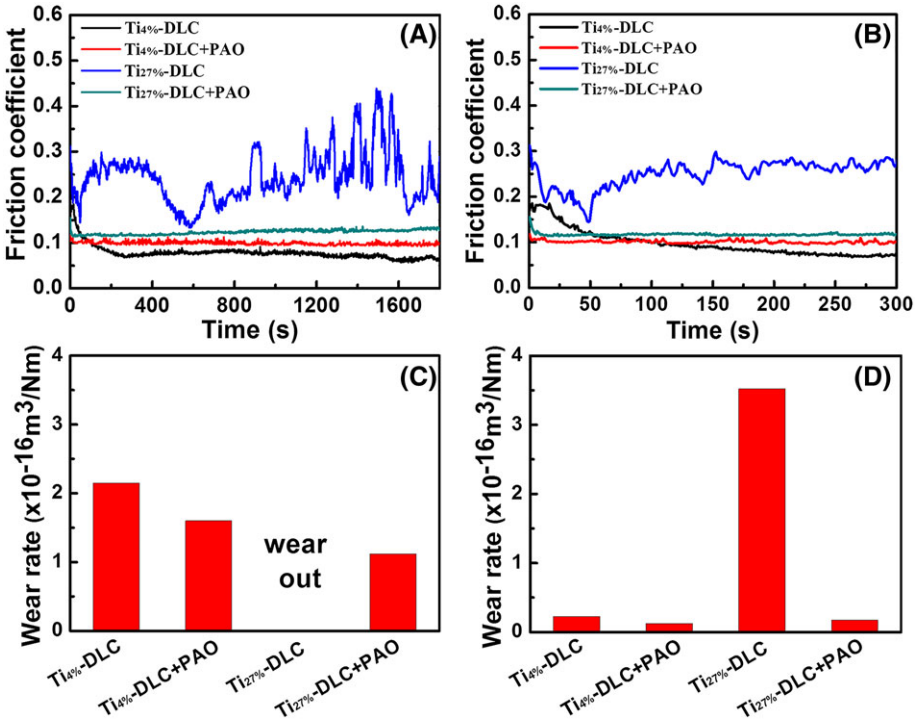

FIGURE 4 (A) Friction sliding curves, (B) friction coefficients of the first 300 seconds, (C) wear rates of $Ti_{4at.\%}$-DLC and $Ti_{27at.\%}$-DLC coatings, and (D) wear rates of steel balls against $Ti_{4at.\%}$-DLC and $Ti_{27at.\%}$-DLC coatings tested under both dry friction and oil lubrication

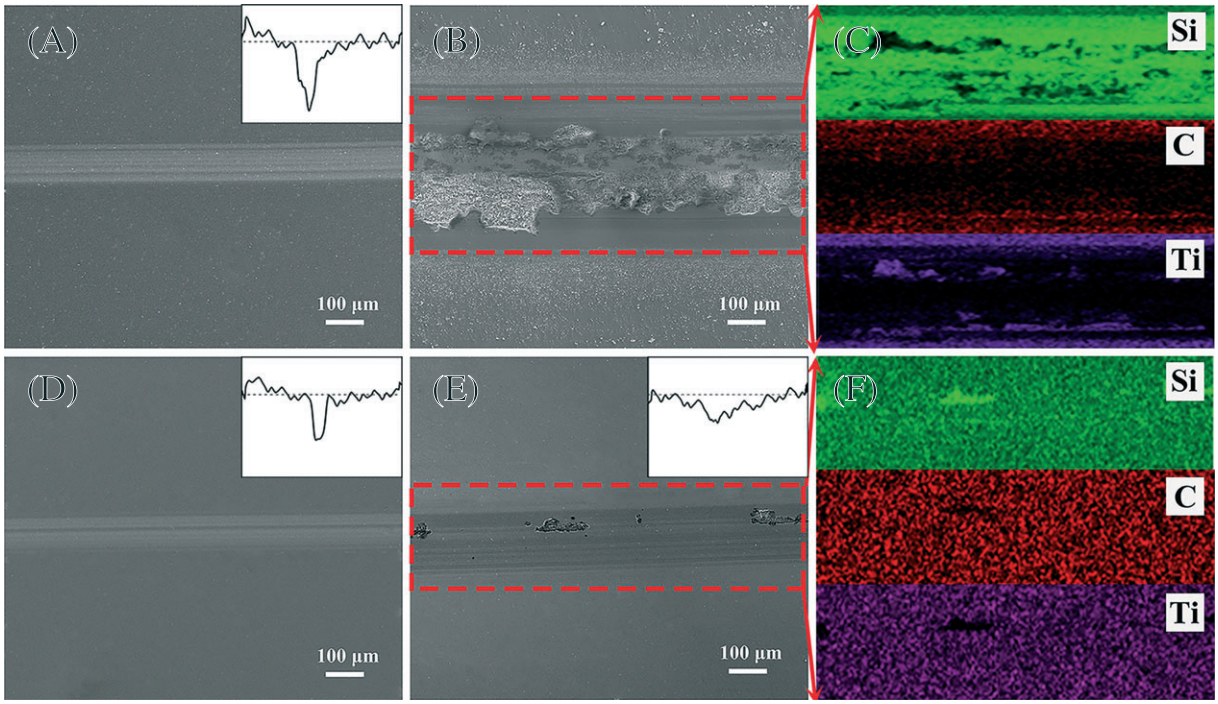

FIGURE 5 SEM micrographs of wear tracks of (A) $Ti_{4at.\%}$-DLC coating tested under dry friction, (B) $Ti_{27at.\%}$-DLC coating tested under dry friction and (C) corresponding EDS mapping, (D) $Ti_{4at.\%}$-DLC coating tested under oil lubrication, and (E) $Ti_{27at.\%}$-DLC coating tested under oil lubrication and (F) corresponding EDS mapping

after friction tests. Generally, Raman spectra of DLC can be normally deconvolved into D peak (breathing vibration mode of sp^2 carbon in aromatic rings) and G peak (stretching vibration mode of all pairs of sp^2 carbon in both aromatic rings and chains)[25]; an increase in the intensity ratio of D peak to G peak (I_D/I_G) indicates the surface graphitization of DLC coatings. Figure 6A shows Raman spectra of the as-deposited $Ti_{4at.\%}$-DLC coating and wear tracks after friction tests under both dry friction and oil lubrication, with a similar I_D/I_G ratio (0.831, 0.827, and 0.828). Figure 6B and 6C exhibits Raman results of the corresponding wear scar after friction tests under both dry friction and oil lubrication, respectively, and the inserted images are optical images of wear scars. In order to deep reveal its difference in

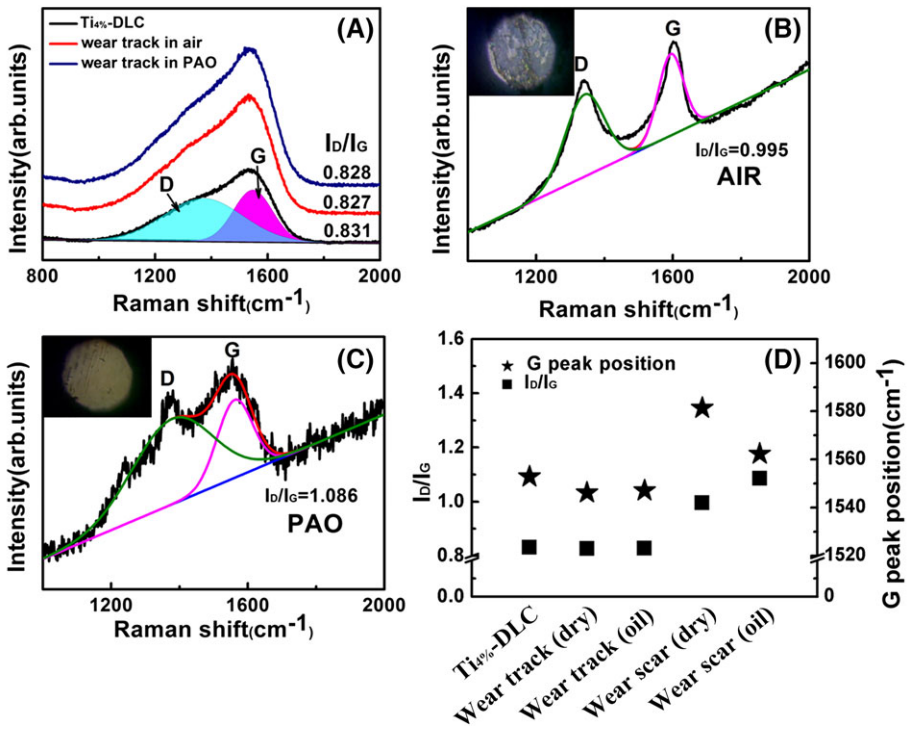

FIGURE 6 Raman spectra of (A) as-deposited $Ti_{4at.\%}$-DLC coating and wear tracks, (B) wear scar on steel ball tested under dry friction, (C) wear scar on steel ball tested under oil lubrication, and (D) I_D/I_G ratio, G peak position under all conditions

component, Figure 6D compares the fitted I_D/I_G ratio value and G peak position of amorphous carbon under all conditions. Compared with as-deposited coating, no distinct difference could be observed in the spectra of wear track, implying a similar carbon atomic bond between wear tracks and as-deposited coating. Besides, Raman spectra with typical amorphous carbon characteristics were observed on wear scar, and compared with as-deposited coating, noted that higher I_D/I_G ratio (from 0.831 to 0.995 and 1.086, respectively) and G peak position (from 1553 to 1581 and 1562 cm^{-1}, respectively) were observed from the wear scar surface under both conditions. The results demonstrated that a friction-induced graphitized carbon layer was formed and transferred from wear track to steel ball due to the easily shear characteristics of the graphite-like lamellar structure, which will not be affected by PAO oil.[26,27]

Figure 7 shows the Raman spectra of the as-deposited $Ti_{27at.\%}$-DLC coating, wear track as well as wear scar after friction tests under oil lubrication. Compared with as-deposited coating, the I_D/I_G ratio of wear track increased from 0.996 to 1.146, and the G peak position shifted to higher wave number, indicating that a graphitized carbon layer was formed on wear track. However, no amorphous carbon signal was observed from wear scar, suggesting that no graphitized carbon layer was transferred to steel ball in this case.

In general, graphitization may occur in the tribological contact because of friction-induced heating under contact and high contact stress.[26] And the formation of graphitized carbon layer can cause an easy slip between the tribo pairs, thereby minimizing friction. However, a higher degree of graphitization and the transfer of graphitized carbon layer will increase the consumption of coating and lead to high wear rate.[28] Therefore, for $Ti_{4at.\%}$-DLC coating, more material will lose from the surface due to transfer of graphitized carbon layer, leading to a slighter higher wear rate (Figure 4) compared with $Ti_{27at.\%}$-DLC coating under oil lubrication.

The above results showed that under oil lubrication condition, the two coatings showed similar tribological behaviors, which may be mainly caused by the oil film formed in the contact area, with theoretical thickness 16 and 6 nm for $Ti_{4at.\%}$-DLC coating and $Ti_{27at.\%}$-DLC coating, respectively, and under dry friction, $Ti_{27at.\%}$-DLC coating was quickly worn out. So, more investigations were performed on the friction results of $Ti_{4at.\%}$-DLC coating in the following section.

Since the tribological properties were closely related to transfer film, we first investigated the component changes in different locations on the wear tracks by SEM and EDS analysis. As shown in Figure 8, three typical positions were selected and characterized, corresponding to the wear debris region (spectrum 1 and 4), wear track region (spectrum 2 and 5), and as-deposited coating (spectrum 3 and 6), respectively, and the atomic percentages of C, O, Ti, and Fe are also present in Table 2. It could be noted that the composition was almost the same between as-deposited coating and wear track, regardless of the test environment. However, the wear debris exhibited distinct compositional variation. As shown in Figure 8A, small pieces of wear deris aggregated around the wear track under dry friction, where a significant increase of O and Fe was observed in spectrum 1, indicating that the steel ball was worn (Figure 4D) and the accumulated debris were mainly composed of ferric oxides. However,

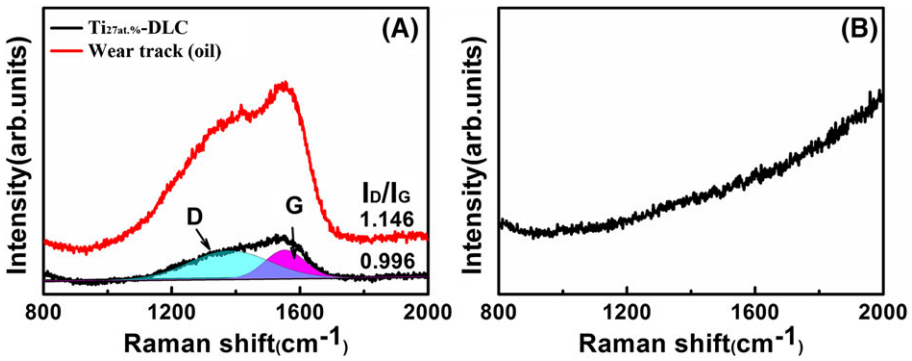

FIGURE 7 Raman spectra from (A) as-deposited $Ti_{27at.\%}$-DLC coating, wear track, and (B) wear scar on steel ball tested under oil lubrication

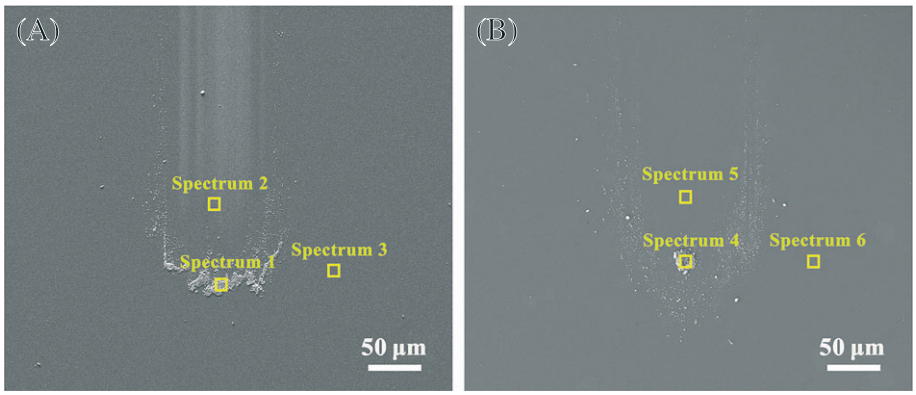

FIGURE 8 Typical positions for EDS test on the wear tracks of $Ti_{4at.\%}$-DLC coatings tested under (A) dry friction and (B) oil lubrication

TABLE 2 Atomic percentages of C, O, Ti, and Fe in the coating surface, wear tracks, and wear debris of $Ti_{4at.\%}$-DLC coatings

Element	C, at.%	O, at.%	Ti, at.%	Fe, at.%	Total, at.%
Spectrum 1	54.40	23.27	4.67	17.66	100.00
Spectrum 2	96.05	0.92	3.03	0.00	100.00
Spectrum 3	94.56	1.29	4.14	0.00	100.00
Spectrum 4	44.63	27.12	26.87	1.38	100.00
Spectrum 5	94.96	1.68	3.36	0.00	100.00
Spectrum 6	94.40	1.87	3.73	0.00	100.00

for the case under oil lubrication shown in Figure 8B, Fe concentration of the accumulated debris (spectrum 4) greatly decreased from 17.66 to 1.38 at.%, and Ti concentration exhibited a significant increase from 4.67 to 26.87 at.%, indicating that there was only slighter abrasion of the steel ball (Figure 4D) and the debris were mainly composed of titanium compound.

The clarification of chemical composition changes of wear scars was also undertaken by SEM and EDS elemental mapping analysis. Under dry friction shown in Figure 9A, the contact area on steel ball was covered with a transfer film, and the corresponding EDS mapping images showed the intensive Ti and O element signals, suggesting that the main ingredient of transfer film might be the oxides of coatings. This result coincided well with the former EDS analysis of the wear tracks, which indicated that the Ti from coating was formed to transfer film due to tribochmical reaction. However, when the test was under oil lubrication condition shown in Figure 9B, there was no obvious transfer film, but only oil stains adhered around the wear scar. In addition, no remarkable signal of Ti and O element emerged. Therefore, it is reasonable to state that titanium compounds will be easily thrown out from the contact area with PAO oil. Clearly, for $Ti_{4at.\%}$-DLC coating, the coating material would be easily transferred to the steel ball and form a stable transfer film under dry friction; however, this process was suppressed by oil to a great extent under oil lubrication.

In order to figure out the chemical composition and chemical bonds of the transfer film, further XPS measurement was performed. Here, XPS analysis was done after 3-minute etching by Ar^+ beam of 2 keV to remove the contamination on surface. Figure 10A and 10C shows the C 1s and Ti 2p XPS spectra of wear scar tested under dry friction. The C 1s spectrum, as shown in Figure 10A, was fitted into four components, that was correlated to sp^2 C—C bond (284.2 eV), sp^3 C—C bond (285.6 eV), C═O bond (288.2 eV),[29,30] and C—Ti bond (282.3 eV).[31] In Ti 2p spectrum (Figure 10C), the peaks at 458.4 and 464.2 eV are usually assigned to the Ti 2p3/2 peak and Ti 2p1/2 peak of TiO, respectively, and the peaks at 456.6 and 462.4 eV are usually attributed to the Ti 2p3/2 peak and Ti 2p1/2 peak of TiC.[31] Hence, the Ti 2p XPS spectra showed that TiC and TiO simultaneously existed in the transfer film, indicating that the Ti from $Ti_{4at.\%}$-DLC reacted with C and O during the friction process. Figure 10B and 10D present the C 1s and O 1s XPS spectra of the wear scars tested under oil lubrication. On account of no Ti 2p peak was observed under this condition, the O 1s peak was analyzed to judge the existence of titanium oxide. The results showed that no Ti-C peak appeared in the C 1s spectra, and it could only be fitted into three peaks corresponding to sp^2 C—C bond (284.5 eV), sp^3 C—C bond (285.3 eV), and C═O bond (288.6 eV), respectively. It should be also noted that there was a strong O 1s peak at about 529.9 eV shown in Figure 10D, which was assigned to ferric oxides instead of titanium oxide.

3.4 | Related mechanism discussion

The H/E and H^3/E^2 ratios are two factors to assess wear-resistant properties and plastic deformation resistance of hard coatings, respectively. Massive titanium carbide nanocrystallites lead to a significant increase in both the hardness and elastic modulus of the $Ti_{27at.\%}$-DLC coating as shown in Table 1. However, the similar H/E ratio shows that the two coatings show similar toughness. The higher hardness and H^3/E^2 ratio of $Ti_{27at.\%}$-DLC imply that the coating has a higher carrying capacity. While it was quickly worn out under dry friction.

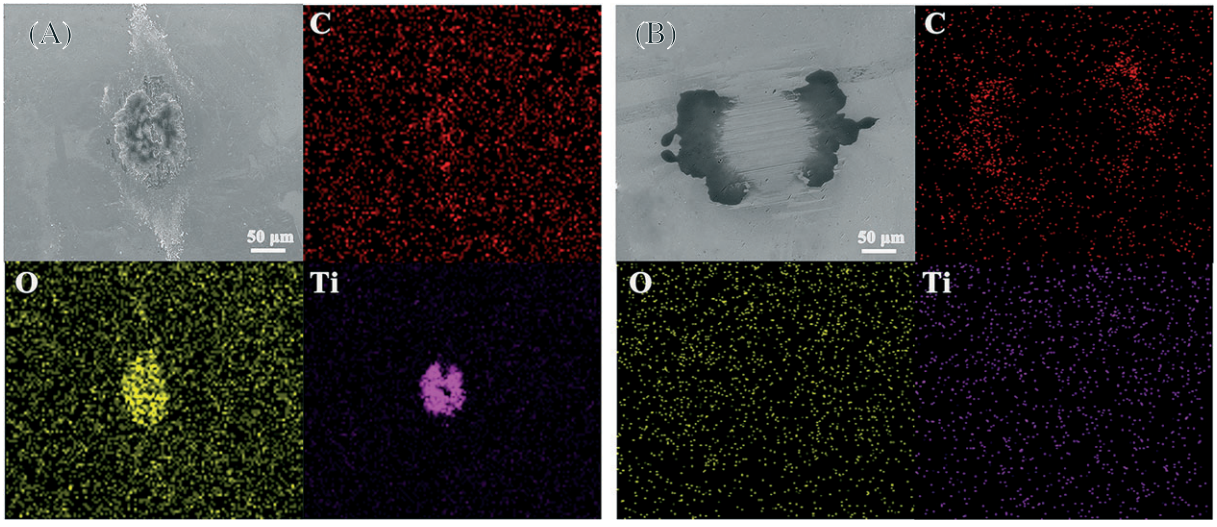

FIGURE 9 SEM and EDS mapping images of the wear scar on the steel balls of $Ti_{4at.\%}$-DLC coatings tested under (A) dry friction and (B) oil lubrication

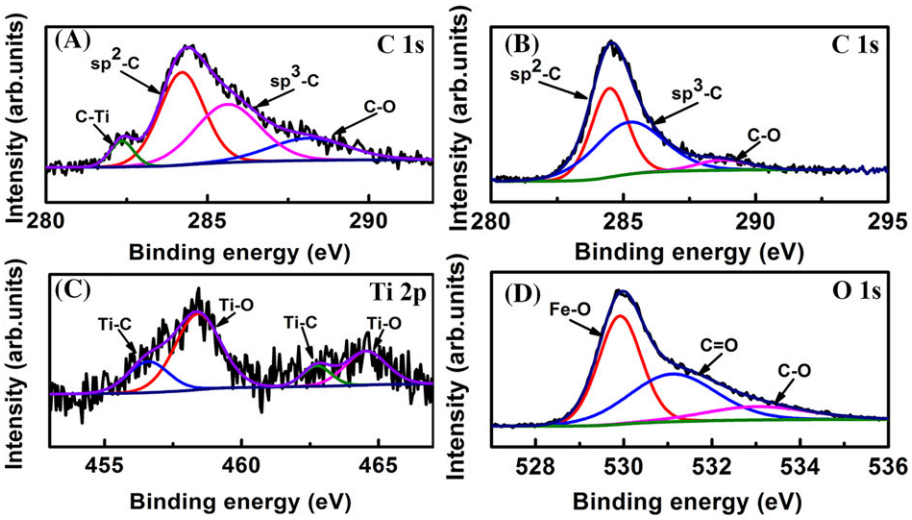

FIGURE 10 XPS results of wear scar on steel balls of $Ti_{4at.\%}$-DLC coating tested under (A), (C) dry friction and (B), (D) oil lubrication

Actually, during friction process, the interaction between wear track and counterpart will decide its tribological behavior, besides the transfer film and PAO oil can also play an important role under different conditions.[21,28] Under dry friction, $Ti_{27at.\%}$-DLC showed serious wear compared with $Ti_{4at.\%}$-DLC coating due to the different microstructures, which have a great influence on mechanical properties and sliding interface. As shown in Figure 11, for $Ti_{4at.\%}$-DLC coating tested under dry friction, there was a run-in period with high friction coefficient (Figure 4A and 4B) due to adhesive wear.[32] The Ti atoms from coating would easily react with C and O to form TiC and TiO hard phase, whereafter aggregating to form transfer film, and then, the transfer film would adhere to steel ball (Figure 9A). It has been certified that the existence of transfer film in sliding interface can effectively decrease friction coefficient and simultaneously protect the underlying coating from further removal.[33,34] In addition, friction-induced graphitization is considered as one of the main causes of low friction because of the graphite-like lamellar structure, which can easily shear between each plane.[27] Therefore, the combined effects of transfer film and graphitization lead to the lowest friction coefficient in steady friction stage when tested under dry friction. With regard to the $Ti_{27at.\%}$-DLC coating, the doped Ti atoms bonded with the surrounding C atoms, and subsequently formed massive carbide nanoparticles that were embedded in the DLC matrix (Figure 3B). A large amount of hard phase compounds of titanium in the sliding interface could lead to large fluctuations of friction coefficient in the running-in peroid (Figure 4A) and serious abrasive wear, even the completely wear of the coating under dry friction. Besides, the microstructure of $Ti_{27at.\%}$-DLC coating would increase the coating compressive stress and promoted the graphitization, which will also accelerate the failure of the coating.[35]

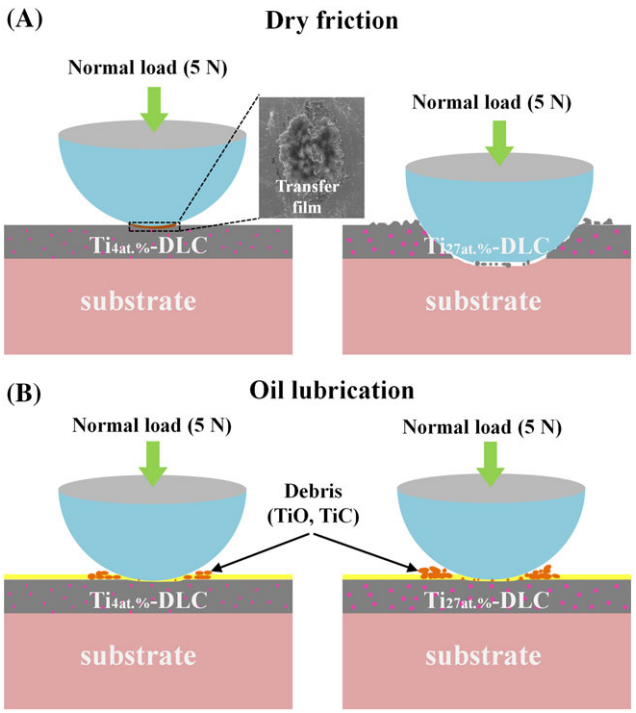

FIGURE 11 A schematic representation of the friction process of $Ti_{4at.\%}$-DLC coating and $Ti_{27at.\%}$-DLC coating under (A) dry friction and (B) oil lubrication.

While, under oil lubrication condition, both coatings showed similar low and stable friction coefficient and the wear rate of coatings and steel balls decreased obviously. Especially for $Ti_{27at.\%}$-DLC coating, PAO oil can greatly improve its tribological properties. The results of oil film thickness indicated that both the two tests were under boundary lubrication. Consequently, both of oil film and transfer film will govern the friction property normally. Different from test in dry friction, the introduction of PAO oil resulted in the more stable friction coefficient curve without run-in period (Figure 4A and 4B). Besides, no transfer film was formed in the sliding interface, and some titanium compound particles were observed around the wear track, as shown in Figures 8B and 9B. This indicated that PAO oil can inhibit the formation of transfer film and throw the TiO and TiC hard particles out from sliding interface, which can account for the lower wear rate of coatings tested in oil lubrication. Besides, compared with $Ti_{4at.\%}$-DLC coating, the absence of the transfer of graphitized carbon layer for $Ti_{27at.\%}$-DLC could reduce the consumption of coating, resulting in the lowest wear rate of $Ti_{27at.\%}$-DLC coating under oil lubrication condition (Figure 4C).

4 | CONCLUSION

Ti-DLC coatings with 4 at.% and 27 at.% Ti content were prepared by a hybrid linear ion beam deposition system. HRTEM results showed that the Ti atoms were dissolved in the DLC matrix for $Ti_{4at.\%}$-DLC coating, while massive titanium carbide nanocrystallites were formed in $Ti_{27at.\%}$-DLC coating. Tribological tests were carried out under dry friction and oil lubrication, respectively. Under dry friction, $Ti_{4at.\%}$-DLC coating showed low friction and wear due to the formation of transfer film and graphitized carbon layer, which all adhered to steel ball, and $Ti_{27at.\%}$-DLC showed serious wear since a large amount of hard phase compounds of titanium in the sliding interface could lead to serious abrasive wear and eventually the failure of the coating. While, under oil lubrication condition, both coatings showed similar low friction and wear due to the existence of oil film (16 nm for $Ti_{4at.\%}$-DLC coating and 6 nm for $Ti_{27at.\%}$-DLC coating) in sliding interface, which can inhibit the formation of transfer film and throw the TiO and TiC hard particles out from sliding interface. And $Ti_{27at.\%}$-DLC coating exhibited lowest wear rate under this condition.

ACKNOWLEDGEMENTS

This work was financially supported by the National Natural Science Foundation of China (51522106,51601211), the National Key R&D Program of China (2017YFB0702303), the Chinese Academy of Sciences President's International Fellowship Initiative (2018VEA0007), the Zhejiang Key Research and Development Program (2017C01001).

ORCID

Youzhi Guo https://orcid.org/0000-0003-0791-1360

REFERENCES

1. Erdemir A, Ramirez G, Eryilmaz OL, et al. Carbon-based tribofilms from lubricating oils. *Nature*. 2016;536(7614):67-71.
2. Kržan B, Novotny-Farkas F, Vižintin J. Tribological behavior of tungsten-doped DLC coating under oil lubrication. *Tribol Int*. 2009;42(2):229-235.
3. Müller M, Ostermeyer GP, Bubser F. A contribution to the modeling of tribological processes under starved lubrication. *Tribol Int*. 2013;64:135-147.
4. Erdemir A. The role of hydrogen in tribological properties of diamond-like carbon films. *Surf Coat Technol*. 2001;146-147:292-297.
5. Vetter J. 60 years of DLC coatings: historical highlights and technical review of cathodic arc processes to synthesize various DLC types, and their evolution for industrial applications. *Surf Coat Technol*. 2014;257:213-240.
6. Zhao F, Li H, Ji L, et al. Effect of microstructural evolution on mechanical and tribological properties of Ti-doped DLC films: how was an ultralow friction obtained? *J Vac Sci Technol A*. 2016;34(3):031504.
7. Li X, Guo P, Sun L, et al. Ti/Al co-doping induced residual stress reduction and bond structure evolution of amorphous carbon films: an experimental and ab initio study. *Carbon*. 2017;111:467-475.
8. Andersson M, Högström J, Urbonaite S, Furlan A, Nyholm L, Jansson U. Deposition and characterization of magnetron sputtered amorphous Cr–C films. *Vacuum*. 2012;86(9):1408-1416.
9. Batory D, Gorzedowski J, Rajchel B, Szymanski W, Kolodziejczyk L. Silver implanted diamond-like carbon coatings. *Vacuum*. 2014;110:78-86.
10. Koh ATT, Hsieh J, Chua DHC. Structural characterization of dual-metal containing diamond-like carbon nanocomposite films by pulsed laser deposition. *Diamond Relat Mater*. 2010;19(5–6):637-642.
11. Cui J, Qiang L, Zhang B, Ling X, Yang T, Zhang J. Mechanical and tribological properties of Ti-DLC films with different Ti content by magnetron sputtering technique. *Appl Surf Sci*. 2012;258(12):5025-5030.
12. Bharathy PV, Nataraj D, Chu PK, et al. Effect of titanium incorporation on the structural, mechanical and biocompatible properties of DLC thin films prepared by reactive-biased target ion beam deposition method. *Appl Surf Sci*. 2010;257(1):143-150.
13. Pei Y, Galvan D, Dehosson J. Nanostructure and properties of TiC/a-C: H composite coatings. *Acta Mater*. 2005;53(17):4505-4521.
14. Haque T, Morina A, Neville A, Kapadia R, Arrowsmith S. Effect of oil additives on the durability of hydrogenated DLC coating under boundary lubrication conditions. *Wear*. 2009;266(1–2):147-157.
15. Haque T, Morina A, Neville A. Influence of friction modifier and antiwear additives on the tribological performance of a non-hydrogenated DLC coating. *Surf Coat Technol*. 2010;204(24):4001-4011.
16. Tasdemir HA, Wakayama M, Tokoroyama T, et al. Ultra-low friction of tetrahedral amorphous diamond-like carbon (ta-C DLC) under boundary lubrication in poly alpha-olefin (PAO) with additives. *Tribol Int*. 2013;65:286-294.
17. Gorbatchev O, Bouchet MIDB, Martin JM, et al. Friction reduction efficiency of organic Mo-containing FM additives associated to ZDDP for steel and carbon-based contacts. *Tribol Int*. 2016;99:278-288.
18. Kano M, Yasuda Y, Okamoto Y, et al. Ultralow friction of DLC in presence of glycerol mono-oleate (GNO). *Tribol Lett*. 2005;18(2):245-251.
19. de Barros'Bouchet MI, Martin JM, Le-Mogne T, Vacher B. Boundary lubrication mechanisms of carbon coatings by MoDTC and ZDDP additives. *Tribol Int*. 2005;38(3):257-264.
20. Kalin M, Roman E, Ožbolt L, Vižintin J. Metal-doped (Ti, WC) diamond-like-carbon coatings: reactions with extreme-pressure oil additives under tribological and static conditions. *Thin Solid Films*. 2010;518(15):4336-4344.
21. Kalin M, Velkavrh I, Vižintin J, Ožbolt L. Review of boundary lubrication mechanisms of DLC coatings used in mechanical applications. *Meccanica*. 2008;43(6):623-637.
22. Kosarieh S, Morina A, Flemming J, Lainé E, Neville A. Wear mechanisms of hydrogenated DLC in oils containing MoDTC. *Tribol Lett*. 2016;64(1).
23. Cai S, Guo P, Liu J, et al. Friction and wear mechanism of MoS2/C composite coatings under atmospheric environment. *Tribol Lett*. 2017;65(3).
24. Ji L, Wu Y, Li H, et al. The role of trace Ti concentration on the evolution of microstructure and properties of duplex doped Ti (Ag)/DLC films. *Vacuum*. 2015;115:23-30.
25. Ferrari AC, Robertson J. Resonant Raman spectroscopy of disordered, amorphous, and diamondlike carbon. *Phys Rev B*. 2001;64(7):075414.
26. Mobarak HM, Masjuki HH, Mohamad EN, et al. Tribological properties of amorphous hydrogenated (a-C:H) and hydrogen-free tetrahedral (ta-C) diamond-like carbon coatings under jatropha biodegradable lubricating oil at different temperatures. *Appl Surf Sci*. 2014;317:581-592.
27. Cui L, Lu Z, Wang L. Probing the low-friction mechanism of diamond-like carbon by varying of sliding velocity and vacuum pressure. *Carbon*. 2014;66:259-266.
28. Al Mahmud KAH, Varman M, Kalam MA, Masjuki HH, Mobarak HM, Zulkifli NW. Tribological characteristics of amorphous hydrogenated (a-C:H) and tetrahedral (ta-C) diamond-like carbon coating at different test temperatures in the presence of commercial lubricating oil. *Surf Coat Technol*. 2014;245:133-147.
29. Wang P, Wang X, Chen Y, Zhang G, Liu W, Zhang J. The effect of applied negative bias voltage on the structure of Ti-doped a-C:H films deposited by FCVA. *Appl Surf Sci*. 2007;253(7):3722-3726.
30. Yamamoto K. Chemical bond analysis of amorphous carbon films. *Vacuum*. 2009;84(5):638-641.

31. Lee NR, Jun YS, Moon KI, Lee CS. Ti-doped hydrogenated diamond like carbon coating deposited by hybrid physical vapor deposition and plasma enhanced chemical vapor deposition. *Jpn J Appl Phys*. 2017;56(3):035506.
32. Shi J, Gong Z, Wang Y, Gao K, Zhang J. Friction and wear of hydrogenated and hydrogen-free diamond-like carbon films: relative humidity dependent character. *Appl Surf Sci*. 2017;422:147-154.
33. Mangolini F, Krick BA, Jacobs TDB, et al. Effect of silicon and oxygen dopants on the stability of hydrogenated amorphous carbon under harsh environmental conditions. *Carbon*. 2018;130:127-136.
34. Czyzniewski A. Characterisation of transfer layer and wear debris on various counterparts sliding against undoped and doped DLC coatings. *Plasma Processes Polym*. 2007;4(S1):S231-S236.
35. Dai W, Ke P, Moon MW, Lee KR, Wang A. Investigation of the microstructure, mechanical properties and tribological behaviors of Ti-containing diamond-like carbon films fabricated by a hybrid ion beam method. *Thin Solid Films*. 2012;520(19):6057-6063.

How to cite this article: Guo Y, Guo P, Sun L, et al. Tribological properties of Ti-doped diamond-like carbon coatings under dry friction and PAO oil lubrication. *Surf Interface Anal*. 2019;51:361–370. https://doi.org/10.1002/sia.6588